

Title: A fNIRS Investigation of Speech Planning and Execution in Adults Who Stutter

Author names and Affiliations:

1. Eric S. Jackson^a, PhD, CCC-SLP (corresponding author)
2. Sobana Wijekumar^b, PhD
3. Deryk S. Beal^{cd}, PhD, CCC-SLP
4. Bryan Brown^e, PhD, CCC-SLP
5. Patricia Zebrowski^f, PhD, CCC-SLP
6. John P. Spencer^g, PhD

Addresses:

^aDepartment of Communicative Sciences and Disorders
New York University
665 Broadway, 9th Floor
New York, NY 10012

^bSchool of Psychology
University of Stirling
Stirling FK9 4LA
Scotland, UK

^cBloorview Research Institute
Holland Bloorview Kids Rehabilitation Hospital
150 Kilgour Road Toronto, Ontario M4G 1R8

^dDepartment of Speech-Language Pathology
Faculty of Medicine, University of Toronto
160-500 University Avenue
Toronto, ON M5G 1V7

^eDepartment of Communication Sciences and Disorders
University of Wisconsin-Eau Claire
239 Water Street
Eau Claire, WI 54702

^fDepartment of Communication Sciences and Disorders
Wendell Johnson Speech and Hearing Center
Iowa City, Iowa 52242

^gSchool of Psychology
Lawrence Stenhouse Building 0.09
University of East Anglia
Norwich, NR4 7TJ, UK

Abstract

Our study aimed to determine the neural correlates of speech planning and execution in adults who stutter (AWS). Fifteen AWS and 15 controls (CON) completed two tasks that either manipulated speech planning or execution processing loads. Functional near-infrared spectroscopy (fNIRS) was used to measure changes in blood flow concentrations during each task, thus providing an indirect measure of neural activity. An image-based reconstruction technique was used to analyze the results and facilitate their interpretation in the context of previous functional neuroimaging studies of AWS that used positron emission tomography (PET) or functional magnetic resonance imaging (fMRI). For planning, we compared neural activity associated with high versus low planning load in AWS and CON. For execution, we compared the neural activity associated with overt versus covert naming in AWS and CON. Broadly, group level effects corroborate previous PET/fMRI findings including under-activation in left-hemisphere perisylvian speech-language networks and over-activation in right-hemisphere homologues. Increased planning load revealed atypical left-hemisphere activation in AWS, whereas increased execution load yielded atypical right fronto-temporo-parietal and bilateral motor activation in AWS. Our results add to the limited literature differentiating speech planning versus execution processes in AWS.

Keywords: stuttering; fNIRS; planning; execution; speech communication; fluency

Highlights

1. This report includes the largest sample of AWS to undergo fNIRS to date.
2. AWS showed atypical activation in left speech-language regions for planning and right hemisphere homologues for execution.
3. Atypical right hemisphere activation comprises a known inhibitory network
4. Group main effects were generally in line with previous PET/fMRI studies of AWS.

Introduction

Stuttering is a neurodevelopmental communication disorder that impacts approximately fifty million adults worldwide. The disorder manifests itself most saliently as intermittent interruptions in the forward flow of speech production including repetitions or audible/inaudible prolongations of sounds and syllables, non-speech compensatory movements (e.g., eye blinking, head/body movements), and communicative avoidance (e.g., choosing to delay or altogether avoid speaking). Living with stuttering can lead to significant frustration and negative social and emotional consequences throughout life (Beilby, Byrnes, Meagher, & Yaruss, 2013; Craig, Blumgart, & Tran, 2009). Significant progress has been made in identifying the neural correlates of stuttering, but a comprehensive brain-based understanding of speech production processes in people who stutter remains elusive. Identifying the neural bases of stuttering has the potential to inform the existing behavioral interventions (for which relapse is common) as well as support the development of neuromodulation techniques that are beginning to be applied to stuttering such as transcranial direct current stimulation (e.g., Chesters, Möttönen, & Watkins, 2018; Yada, Tomisato, & Hashimoto, 2018).

The neural correlates of typical speech motor control have been well documented using functional neuroimaging studies of unimpaired control participants via positron emission tomography (PET) and functional magnetic resonance imaging (fMRI). At the most basic level, the cortical neural network for speech during overt syllable and single word production involves the frontal, motor, parietal, and temporal cortices. Specifically, the inferior frontal gyri (IFG), precentral and postcentral gyri

(preCG/postCG), supplementary motor area (SMA), supramarginal gyri (SMG), inferior parietal lobule (IPL), and superior temporal gyri (STG) are routinely active during overt syllable and/or single word production (Bohland & Guenther, 2006; Price, 2012; Riecker, Brendel, Ziegler, Erb, & Ackermann, 2008; Shuster & Lemieux, 2005; Sörös et al., 2006).

There is also a relatively large PET and fMRI literature detailing atypical activation throughout the speech motor control network of adults who stutter (AWS) relative to unimpaired controls (CON) during overt syllable and word production, including: 1) reduced activation in left fronto-temporal and perisylvian networks (e.g., IFG and STG) (Chang, Horwitz, Ostuni, Reynolds, & Ludlow, 2011; De Nil, Kroll, Kapur, & Houle, 2000; Fox et al., 2000; Jiang, Lu, Peng, Zhu, & Howell, 2012; Neumann et al., 2004); 2) increased activation in right frontal-parietal regions (e.g., IFG, SMA, and postCG) (De Nil et al., 2000; De Nil, Kroll, Lafaille, & Houle, 2004; Kell et al., 2009; T. Loucks, Kraft, Choo, Sharma, & Ambrose, 2011; Neumann et al., 2004; Preibisch et al., 2003; Sakai, Masuda, Shimotomai, & Mori, 2009); and 3) atypical functional connectivity between preCG and IFG, superior frontal gyrus (SFG), and SMA (Chang et al., 2011).

The experimental tasks used in previous work involved oral reading or picture naming, both which allow for gross examination of and broad conclusions about the neural correlates of speech motor control. However, speech motor control encompasses neural regions associated with both the planning and execution of speech movements, where planning refers to the assembling of a temporally-specified, physical control structure associated with specific vocal tract movements (Mooshammer et al., 2012) and execution refers to the overt realization of these movements (i.e., articulation). The initiation of planning necessarily precedes the initiation of execution,

but planning and execution may overlap in time, particularly during tasks that involve speech production at a syllable level or higher (i.e., with multiple segments). For this reason, to advance our understanding of the neural mechanisms underlying speech motor control in stuttering it is critical to address the overlap between planning and execution processes when designing tasks that attempt to differentiate planning and execution.

The relative contribution of planning and execution remains an open question of significant importance to understanding both the key neural correlates of stuttering onset and development, and those essential to successful treatment. To date, only two studies have attempted to isolate speech motor planning and execution in AWS. In the first, Chang, Kenney, Loucks, and Ludlow (2009) examined planning and execution within the same task by separating these processes temporally and using fMRI with sparse sampling. Participants were aurally presented two successive syllables and instructed to arrange the syllables in the same or reverse order (planning) before repeating them (execution) following a “go” signal. During planning, the AWS exhibited reduced activation compared to the CON in motor and parietal regions including bilateral preCG and IPL. During execution, the AWS exhibited atypical activity in fronto-temporal and motor regions including greater activation in R-IFG, R-STG, R-preCG, and less activation in L-STG, compared to the CON.

In the only other study to examine differences in speech motor planning and execution in AWS versus CON, Lu and colleagues (2010) implemented a task with three speaking conditions: 1) non-repeated, single syllable non-words; 2) repeated single-syllable non-words—essentially a three-syllable non-word with identical syllables;

and 3) three-syllable non-words with different syllables. The stimuli were created to allow experimental manipulation of planning load (comparing conditions 2 and 3) and execution load (comparing conditions 1 and 2). The planning contrast revealed that the AWS exhibited atypical activity compared to the CON in fronto-temporal and motor regions including increased activation in bilateral middle and superior frontal gyri (MFG/SFG), IFG, and postCG, and reduced activity in L-STG and right medial frontal gyrus (Lu, Chen, et al., 2010, supplementary material). During execution, the AWS exhibited increased activity compared to the CON in bilateral IFG and MFG, L-postCG, R-STG, and R-SFG, and reduced activity in left anterior middle temporal gyrus (MTG) (Lu, Chen, et al., 2010, supplementary material). The planning contrast in Lu et al. sufficiently isolated speech motor planning through a comparison of productions for which the only variable to change was planning load. However, it may not have sufficiently isolated execution because one vs. three-syllable productions differ in planning load (i.e., the temporally-specified control structure [“the plan”] is less complex for one vs. three syllable productions); as a result, the execution phase may have been contaminated by planning processing.

To expand upon these earlier investigations, we used two tasks to assess planning and execution in AWS and CON. These tasks measured the difference between high and low planning and execution load. To examine planning, we implemented the planning task from Lu et al. (2010). This task isolated planning by contrasting the neural activity associated with two conditions in which the only difference was the level of planning load (high and low). To isolate execution, we implemented an overt vs. covert naming task thereby contrasting the level of execution

load. To study these processes during speech production, we used functional near-infrared spectroscopy (fNIRS).

fNIRS is an optical imaging technology that measures light absorption in the brain, particularly by oxy-hemoglobin (HbO) and deoxy-hemoglobin (HbR), providing an indirect measure of neural activity (Ferrari & Quaresima, 2012). While fNIRS provides lower spatial resolution and cortical coverage than fMRI, it does offer several advantages. It is less sensitive to movement, silent during data acquisition, and portable, and therefore more conducive to testing in natural speaking environments in which participants are able to sit upright and speak. In addition, fNIRS is significantly less expensive to purchase, operate and maintain than other commonly used techniques (e.g., PET/fMRI). Few studies have leveraged the advantages offered by fNIRS to study speakers who stutter. In a pilot study, Tellis, Vitale, and Murgallis (2015) examined two AWS and two CON during reading, counting, and free speech. The AWS exhibited atypical neural activation in Broca's and Wernicke's areas, as well as R-IFG across the tasks (Tellis et al., 2015). In a larger and more recent study, Walsh, Tian, Tourville, Yücel, Kuczek, and Bostian (2017) used fNIRS with children who stutter (CWS) and CON (aged 7-11 years) during connected speech. Walsh et al. found reduced activation in CWS in L-IFG and left premotor cortex during speech production (i.e., picture description), which is consistent with widely reported findings of reduced activity in left hemisphere perisylvian speech-language regions (Chang et al., 2011; De Nil et al., 2000; Fox et al., 2000; Jiang et al., 2012; Neumann et al., 2004).

Our current study aimed to use fNIRS to examine the discrete neural correlates of speech motor planning and execution in AWS. To accomplish this, we implemented

two tasks that isolated these processes: the Lu et al. (2010) task isolated planning by comparing the neural activity associated with two conditions that changed only in planning load, and our novel execution task that isolated execution by comparing the neural activity associated with two conditions that changed only in execution load (i.e., overt vs. covert production). We used an image-based fNIRS analysis that allowed us to compare spatial maps of our results to those from previous PET and fMRI studies through consistent registration of cortical regions across participants and reporting of results in voxel space within the brain volume (e.g., Eggebrecht et al., 2014; Perlman, Huppert, & Luna, 2015; Wijekumar, Huppert, Magnotta, Buss, & Spencer, 2017). We designed a probe geometry such that 36 channels overlaid important ROIs within the speech motor network. By doing so, we achieved increased cortical coverage compared to previous fNIRS studies of stuttering, while preserving a focused approach based on the relevant literature. To our knowledge, our study is the largest fNIRS study of AWS to date.

Experimental procedures

Participants

All procedures were approved by the University of Iowa Institutional Review Board on Human Subjects. Fifteen AWS (four female) and 15 CON (three female) were recruited through clinical referrals and the University of Iowa community (AWS: $M = 27.07$, $SD = 8.15$; CON: $M = 26.07$, $SD = 3.45$). Participants were right-handed, monolingual speakers of English. The AWS were included if they were rated greater than 1 by a speech-language pathologist with expertise in the assessment and treatment of stuttering on the 0-7 Iowa Scale of Severity of Stuttering (Johnson, Darley,

& Spriesterbach, 1963), and either (1) described their speech as containing stuttering-like disfluencies (as defined by Yairi & Ambrose, 1992) in a communication history questionnaire or (2) received a diagnosis of stuttering from an American Speech-Language-Hearing Association certified speech-language pathologist. Clinician severity ratings on the 0-7 Iowa Scale included: three ratings of 2, two ratings of 3, six ratings of 4, and four ratings of 5. All participants were screened for hearing and visual impairment, and reported negative histories of speech-language (other than stuttering) and neurological disorders.

Tasks and Stimuli

Speech Motor Planning

The planning task from Lu et al. (2010) was implemented to manipulate planning load. The stimuli consisted of non-words that varied in their degree of planning load (high vs. low) with level of execution load held constant (i.e., three syllables). The low planning load non-words were comprised of the same three syllables (same syllable non-words; SSN) whereas high planning load non-words were comprised of three different syllables (different syllable non-words; DSN). The phonotactic complexity of the non-words, as determined by taking the sum of the biphone probabilities using an online phonotactic probability calculator (Vitevitch & Luce, 2004) did not significantly differ between SSN and DSN stimuli ($t[19] = 1.079$ $p = 0.28$). Stimuli are presented in Appendix A. In total, 20 SSN and 20 DSN were included. Each non-word was produced once, and 15 SSN and 15 DSN were randomly selected to be produced twice (for a total of 70 trials). Participants produced 35 SSN and 35 DSN, in seven blocks of ten words each, and were given a brief rest between blocks. Accuracy and fluency judgments

were marked online by the examiner. Figure 1A depicts the timescale of the planning task.

Speech Motor Execution

A picture-naming task during which participants named pictures either aloud (overt) or silently without articulation (covert) was implemented to isolate processes associated with speech execution. For covert production, participants were given explicit instructions to ensure that words were produced silently, without moving their articulators (i.e., “Say it in your head”). These instructions increased the probability that participants produced the words silently, as opposed to inhibiting them. Forty-two photographs from the Hatfield Image Test (Adlington, Laws, & Gale, 2009), each on a white background, were used as stimuli. All pictures represented nouns and were developmentally appropriate (i.e., acquired by age five). Pictures were pseudo-randomly selected to be overt or covert. The picture border was black until it either turned green (for overt naming) or red (for covert naming). Twelve pictures were presented in each of seven blocks, for a total of 84 trials. Forty-two words were monosyllabic and 42 were multisyllabic (i.e., two or three syllables). During pilot testing, one participant commented that near the end of the experiment he was able to predict whether repeated words were going to be overt or covert (e.g., if the word was already produced overtly, he knew before the go signal that he would be required to produce the word covertly). As a result, eleven foils were introduced (i.e., the overt-covert pairs were different), which reduced the predictability of the task. Figure 1B depicts the timeline of the execution task. Accuracy and fluency were determined online by a speech-language pathologist with expertise in stuttering assessment and intervention (author BB).

Experimental Procedure

Participants were seated in a chair approximately 24 inches from a television monitor. Stimuli were presented via E-Prime, which also registered behavioral responses (i.e., correct, incorrect, disfluent, marked by the examiner). Verbal responses were recorded with a Phillips DV1400/00 digital recorder and a Phillips 9173 lapel microphone. The fNIRS cap was centered so that the Cz location was on a line extending from theinion to the nasion at the intersection of a line extending from the left to the right peri-auricular points. After the cap was positioned, it was secured in place with a hook-and-loop strap and optodes were placed into grommets housed within the fabric of the cap. The scalp landmarks and positions of the optode geometry were digitized using a Polhemus Patriot Motion sensor before the tasks began.

fNIRS Recording and Processing

Instrumentation and cap design

A TechEn CW6 system with 12 sources and 24 detectors and wavelengths at 830 nm and 690 nm was used (sampling rate 25Hz). The probe geometry consisted of 36 channels covering parts of the frontal, motor, parietal, and temporal cortices (see Figure 2). These regions were selected based on the results of six published research reports that used fMRI to examine speech production in AWS (Chang et al., 2009; Lu, Chen, et al., 2010; Lu et al., 2009; Neumann et al., 2003; Preibisch et al., 2003; Watkins, Smith, Davis, & Howell, 2008). Regions were averaged into a single ROI if their coordinates were within one centimeter of one another. Of the 36 channels, four were short source-detector channels, which were used for removing signals from the scalp and skull. The probe geometry was optimized following the methodology detailed

in Wijekumar et al. (2015). The positions of the sources and detectors were anchored to the 10-20 system of electrode placement, so that the probe geometry could be scaled up or down to fit caps of different head sizes and record from the same cortical regions across participants (see Wijekumar et al., 2015).

Pre-processing fNIRS data

Data were processed using HOMER2 (www.nmr.mgh.harvard.edu/PMI/resources/homer2). Signals were converted from raw intensity values to optical density units. Motion artifacts were detected using the *MotionArtifactbyChannel* function (tMotion = 0.5, tMask = 1.0, StdevThresh = 50 and AmpThresh = 5) and noisy segments were corrected using targeted principal components analysis [nSV = 0.97, maxIter=5] (Yücel, Selb, Cooper, & Boas, 2014). Motion artifact correction was run a second time to identify any remaining noisy segments and rejected using the *StimRejection* function. The data were then band-pass filtered to include frequencies between 0.016 Hz and 0.5 Hz. Optical density data were converted to concentration units using the modified Beer-Lambert law. Separate general linear models were run on HbO and HbR concentrations for each task. Each regressor was constructed by convolving a modified gamma function with a square wave of duration of 10 s. For the planning task, the onset of the regressor was speech initiation. For the execution task, the onset of the regressor was the “go” signal, when the color of the picture frame changed from black to red or green. A beta estimate was obtained for each condition, channel, chromophore, and participant.

Forward model for fNIRS image reconstruction

The Colin adult template, included with the HOMER2 analysis software, was used to generate the forward model for fNIRS image reconstruction. The Colin template was segmented into separate volumes for gray matter, white matter, cerebrospinal fluid and scalp tissues using the *3dSeg* function in AFNI (Analyses of Functional NeuroImaging). These volumes were converted into a format that could be imported into *AtlasViewer* in HOMER2. This procedure was described fully in Wijekumar et al. (2017).

Digitized scalp landmarks and source and detector positions from each participant were projected onto the adult and child atlases to create participant-specific atlases. Monte Carlo simulations were run with 100 million photons to create sensitivity profiles for each channel of the probe geometry (Wijekumar, Huppert, et al., 2017). These sensitivity profiles were converted to NIFTI format using AFNI (www.afni.nimh.nih.gov) and then summed together and thresholded to include voxels with an optical density of 0.0001 or greater (see Wijekumar et al., 2015 for justification). These images were masked for each participant. Each participant-specific mask was transformed to the space of the original atlas (using *3dAllineate* in AFNI) and then summed together to create a group mask. The group mask was thresholded such that only those voxels with data from all adults were included. The mask was then transformed to the Montreal Neurological Institute (MNI) space using *3dAllineate*.

Image Reconstruction

Methods for image reconstruction using fNIRS and similar optical approaches have been described in detail elsewhere (Eggebrecht et al., 2014; Hirsch, Adam Noah, Zhang, Dravida, & Ono, 2018; Perlman, Huppert, & Luna, 2016; Putt, Wijekumar,

Franciscus, & Spencer, 2017; Wijekumar, Huppert, et al., 2017; Wijekumar, Magnotta, & Spencer, 2017). Briefly, after accommodating for the forward model and beta coefficients (explained in the previous section), the relationship between the hemodynamic response and delta optical density is given by:

$$\begin{bmatrix} d \cdot \varepsilon_{HbO}^{\lambda 1} \cdot \beta_{HbO} + d \cdot \varepsilon_{HbR}^{\lambda 1} \cdot \beta_{HbR} \\ d \cdot \varepsilon_{HbO}^{\lambda 2} \cdot \beta_{HbO} + d \cdot \varepsilon_{HbR}^{\lambda 2} \cdot \beta_{HbR} \end{bmatrix} = \begin{bmatrix} \varepsilon_{HbO}^{\lambda 1} \cdot F^{\lambda 1} & \varepsilon_{HbR}^{\lambda 1} \cdot F^{\lambda 1} \\ \varepsilon_{HbO}^{\lambda 2} \cdot F^{\lambda 2} & \varepsilon_{HbR}^{\lambda 2} \cdot F^{\lambda 2} \end{bmatrix} \cdot \begin{bmatrix} \Delta HbO_{vox} \\ \Delta HbR_{vox} \end{bmatrix}$$

where F represents the channel-wise sensitivity volumes from the Monte Carlo simulations. ΔHbO_{vox} and ΔHbR_{vox} are voxel-wise relative changes in HbO and HbR concentrations and need to be estimated using the image reconstruction approach. We can re-write this equation as:

$$Y = L \cdot X$$

where

$$Y = \begin{bmatrix} \beta_{dOD}^{\lambda 1} \\ \beta_{dOD}^{\lambda 2} \end{bmatrix}, L = \begin{bmatrix} \varepsilon_{HbO}^{\lambda 1} \cdot F^{\lambda 1} & \varepsilon_{HbR}^{\lambda 1} \cdot F^{\lambda 1} \\ \varepsilon_{HbO}^{\lambda 2} \cdot F^{\lambda 2} & \varepsilon_{HbR}^{\lambda 2} \cdot F^{\lambda 2} \end{bmatrix} \text{ and } X = \begin{bmatrix} \Delta HbO_{vox} \\ \Delta HbR_{vox} \end{bmatrix}$$

Solving for X yields voxel-wise maps of relative changes in concentration for each condition, channel, participant and chromophore. These voxel-wise maps are transformed to MNI space and then multiplied with the thresholded group masks.

Group Analyses

Behavioral Analyses

Inaccurate and stuttered trials were excluded from the fNIRS analyses. For the planning task, inaccurate trials were defined as any trial including altered or omitted syllables or altered syllable sequence, as well as interjections, fillers, or revisions. Trials were also excluded from the analyses if the participant initiated a speech act immediately after repeating the stimuli. For the execution task, overt trials were

inaccurate if the item in the picture was not named accurately. Obvious synonyms were considered to be correct (e.g., “hamburger”/“cheeseburger” and “couch”/“sofa”). Covert trials were considered to be incorrect only if the participant produced speech. Stuttered trials were excluded from the analyses to reduce movement artifact due to stuttering behaviors and to reduce noise in the data due to non-task oriented behavior, as is common practice in the stuttering literature. Stuttered trials (i.e., stuttering-like disfluencies) were comprised of part-word repetitions, prolongations, or blocks.

fNIRS Analyses

Four separate ANOVAs were run using the 3dMVM function from AFNI: planning HbO; planning HbR; execution HbO; execution HbR. Each ANOVA had one between-subjects factor of Group (AWS vs. CON) and one within-subjects factor of Condition (SSN vs. DSN for planning and overt vs. covert for execution). The main effect and interaction images were thresholded to correct for family-wise errors (voxel-wise threshold of $p < 0.05$, $\alpha < 0.05$, voxel size of 8 mm^3 and a cluster size of 10 voxels). Voxels with a significant interaction effect were interpreted at the interaction level and main effects within these same voxels were ignored. Next, to address our goal to compare brain activity between AWS and CON, we focused on the group main effect for any voxels that had both a main effect of group and a main effect of condition. This resulted in the exclusion of a total of 3,586 voxels across all of the condition main effects. Average beta values from all remaining voxels were extracted for each condition, participant and chromophore from each of the clusters in the final main effects and interactions maps. Separate post-hoc comparisons for each chromophore in each cluster that demonstrated a significant GroupXCondition interaction were conducted.

Since we were most interested in the AWS and AWS/CON comparisons, we focused on the Group main effects and the GroupXCondition interactions. For completeness, results from the main effect of Condition are reported in Appendix C.

The hemodynamic response function for fNIRS reflects an inverse relationship between HbO and HbR such that an increase in HbO is generally accompanied by a decrease in HbR. There is much debate surrounding the nature of the relationship between HbO and HbR. For readability and ease of interpretation, the results of the current study will be presented such that an increase in HbO or decrease in HbR is referred to as an *increase* in neural activation. This approach follows trends observed in previous papers (e.g., Dravida, Noah, Zhang, & Hirsch, 2017; Strangman, Culver, Thompson, & Boas, 2002; Zhang, Noah, Dravida, & Hirsch, 2017; Zhang, Noah, & Hirsch, 2016). HbO and HbR will be combined in all tables and figures.

Results

Behavioral Results

During the planning task, the AWS produced more inaccurate and stuttered trials than the CON ($t[42]=2.37, p < .05$; $t[35]=2.54, p<.05$, respectively). The GroupXCondition interaction was not significant for accuracy ($t[27]=.55, p>.05$), but approached significance for fluency ($t[27]=2.04, p=.051$). Post-hoc testing revealed that the AWS produced more disfluent utterances than the CON for DSN ($t[27]=1.92, p=.06$) but not SSN. For the execution task, significant differences were not found between groups for accuracy or fluency ($t[56]=.10, p>.05$; $t[56]=.13, p>.05$, respectively). A significant GroupXCondition interaction was found for fluency ($t[56]=2.15, p<.05$) but not for accuracy ($t[28]=1.67, p>.05$). Post-hoc testing revealed that the AWS produced

significantly more disfluencies than the CON during the overt condition ($t[28]=2.26$, $p<.05$), as expected.

fNIRS Results

Significant clusters that survived familywise correction are presented in Tables 1 and 2 (for planning and execution, respectively).

Group main effects

Group main effects pooled across both task ANOVAs and chromophores (HbO, HbR; for details, see Tables 1 and 2) are shown in Figure 3A. As Figure 3A indicates, the AWS in this study exhibited atypical activation, compared to the CON, in bilateral frontal-parietal networks and motor regions. Specifically, the AWS exhibited greater activation (red) in R-IFG, R-MFG, R-SMG, and R-postCG, and lesser activation (light green) in L-IFG, L-preCG, and L-postCG, compared to the CON. Figure 3B shows averaged hemodynamic response functions (HRFs) that correspond to two of these clusters (R-IFG, R-postCG). We have identified channels that overlaid these clusters in the majority of our participants and extracted and displayed HRFs for CON and AWS. Consistent with the image-based analysis, AWS showed greater activation (higher concentrations of HbO) in channels overlying R-IFG and R-postCG.

Planning

Significant GroupXCondition interactions for the planning task (SSN vs. DSN) were observed for clusters in frontal networks including bilateral IFG and L-MFG (see Table 1). Post-hoc comparisons (both within-group and within-condition) were conducted for all clusters with significant interactions. The CON showed greater activation (dark green) in L-IFG for the high vs. low load condition ($F[2,27] = 4.88$, $p =$

.036, $d = .80$) (see Figure 4A), while the AWS did not exhibit this pattern. No other post-hoc comparisons yielded significant results.

Execution

Significant GroupXCondition interactions were observed for clusters in right fronto-temporo-parietal networks including R-SMG, R-STG, and R-IFG, as well as motor regions bilaterally (see Table 2). As shown in Figure 4B, post-hoc comparisons revealed that the AWS exhibited greater activation (red) in R-SMG during the covert vs. overt condition ($F[2,28] = 5.78$; $p = .023$, $d = .88$), whereas the CON did not exhibit this pattern. The CON exhibited greater activity (purple) in R-IFG ($F[2,28] = 6.25$; $p < .05$, $d = .43$) and R-STG ($F[2,28] = 5.82$; $p < .05$, $d = .88$) during covert vs. overt production. In addition, the AWS exhibited greater activation (light green) in R-postCG ($F[2,28] = 7.10$; $p < .05$, $d = .97$) and L-preCG ($F[2,28] = 5.25$; $p < .05$, $d = .76$) during the overt vs. covert condition (Figure 4B); the CON did not exhibit these patterns. No other post-hoc comparisons yielded significant results.

Discussion

The primary goal of our study was to determine the neural correlates of speech planning and execution in AWS and CON using fNIRS. Compared to CON, the AWS in our study exhibited significant atypical activation patterns related to both speech motor planning and execution processing. Differences in planning were associated with atypical activity in left frontal networks, whereas execution differences were associated with atypical activity in right fronto-temporo-parietal networks, as well as left motor regions.

Neural Correlates of Planning in Adults Who Stutter

We found higher neural activation in the L-IFG in CON with higher planning load but no such change in neural activation for AWS. The atypical activation of L-IFG during speech-motor planning is consistent with previous functional imaging studies of AWS (Braun et al., 1997; De Nil et al., 2008; Lu, Chen, et al., 2010; Lu et al., 2009; Neumann et al., 2003; Watkins et al., 2008). It is also well documented that the anatomical development of L-IFG is atypical in children who stutter as young as 3 to 7-years-old (Beal, Gracco, Brettschneider, Kroll, & Luc, 2013; Chang, Erickson, Ambrose, Hasegawa-Johnson, & Ludlow, 2008; Garnett et al., 2018) and continues along an abnormal trajectory into middle-age adulthood for those with persistent forms of the disorder (Beal et al., 2015). Studies of normal speech processes have demonstrated that the L-IFG is active during the internal construction of a speech-motor plan including phonetic encoding and syllabification (Heim, Eickhoff, & Amunts, 2009; Indefrey & Levelt, 2004; Papoutsi et al., 2009; Schuhmann, Schiller, Goebel, & Sack, 2009). Our results indicate that, at least intermittently, AWS do not recruit the necessary neural resources for the planning of utterances of increased complexity. Salmelin, Schnitzler, Schmitz, and Freund (2000) leveraged the high temporal resolution of magnetoencephalography to document the time course of neural events during speech-motor planning in AWS and CON. Salmelin et al. found that rather than the typical pattern of activity starting in L-IFG, advancing to left lateral central sulcus, and then to the dorsal premotor cortex, AWS had activity first arising in motor cortex prior to L-IFG thus indicating attempts to initiate the motor programs prior to the construction of the articulatory plan. In addition, the front aslant tract (i.e., between Broca's and SMA) has been implicated as a neural correlate of stuttering (Kronfeld-Duenias, Amir, Ezrati-

Vinacour, Civier, & Ben-Shachar, 2016; Misaghi, Zhang, Gracco, Luc, & Beal, 2018; Qiao et al., 2017), highlighting the possible dysfunction between planning/execution areas in stuttering speakers. Taken together with previous results from the literature, our findings confirm the importance of the L-IFG for our understanding of stuttering and indicate involvement of neural processes underlying speech-motor planning in the disorder.

Execution

That the CON exhibited greater neural activity in R-IFG during the covert vs. overt condition, while the AWS did not exhibit this pattern, suggests that execution processes (and not planning processes) may be responsible for the right lateralization often reported for AWS. R-IFG has been designated a “neural signature” of stuttering, and has been shown to exhibit atypical activity in AWS in covert and overt speech production at the single word through paragraph level (Brown, Ingham, Ingham, Laird, & Fox, 2005; Budde, Barron, & Fox, 2014). This result is in line with Chang et al. (2009) who found increased activation in R-IFG in AWS during their execution contrast, but not during their planning contrast. Our interpretation however is at odds with that of Lu et al. (2010) who concluded that atypical planning was responsible for the rightward shift in activation, reflective of compensation for L-IFG under-activation. The execution task in the current study differed from that in the Lu et al. (2010) study, in which execution was determined by comparing activity associated with one-syllable and three-syllable word productions, which does not isolate execution processing because one- vs. three-syllable words require different levels of motor planning. In the current study, the

execution task required covert vs. overt production of words matched for syllable number. Thus, planning was held constant while execution load changed.

R-IFG is part of a network including R-SMG that underlies response inhibition and execution (Aron & Poldrack, 2006; Aron, Robbins, & Poldrack, 2004; W. Cai, Ryali, Chen, Li, & Menon, 2014; Hartwigsen, Neef, Camilleri, Margulies, & Eickhoff, 2018). Recall that the AWS in the present study exhibited greater activation than the CON across tasks (planning, execution) in R-IFG and R-SMG, which indicates a general over-activation in this network. The execution contrast revealed that the atypical activation is due to execution because there were no between-group differences for the planning contrast in either R-IFG or R-SMG. R-IFG and R-SMG are also part of the ventral frontoparietal network which is involved in the detection of and re-orientation following behaviorally relevant stimuli (in the current study, the “go” signal) (Corbetta, Kincade, & Shulman, 2002), and the rightward shift apparent here is in line with previous re-orienting studies (Arrington, Carr, Mayer, & Rao, 2000; Corbetta, Kincade, Ollinger, McAvoy, & Shulman, 2000). The CON exhibited the expected reduction in R-IFG activity during the overt condition, whereas the AWS did not, suggesting weaker inhibition or over-activation when given the signal to produce speech overtly. Interestingly, the AWS exhibited greater R-SMG activation during the covert condition, while the CON did not exhibit this pattern. It is possible that within this inhibitory network, R-SMG plays a compensatory role in inhibiting motor responses—that is, compensating for the lack of inhibition in R-IFG during overt speech production. These claims warrant further testing.

Inhibition in Stuttering

The broad claim that the inhibitory network plays an important role in stuttering has been made previously (Aron, Behrens, Smith, Frank, & Poldrack, 2007). We take our findings to suggest, as Neef et al. (2018) speculated, that inhibitory networks, particularly those involved in *proactive* inhibition (Vanderhasselt, Kühn, & De Raedt, 2013) are central to the phenomenon of stuttering anticipation, or one's awareness that she/he will stutter on upcoming sounds, syllables or words if the associated speech plan is executed without alterations (e.g., stalling, circumlocution, word substitution). Anticipation of stuttering is pervasive in AWS, and by definition occurs at the level of speech motor planning prior to execution (Jackson, Yaruss, Quesal, Terranova, & Whalen, 2015). Subsequently, the speaker becomes aware, at least some of the time, that if he continues speaking, he will produce stuttered speech. It may be the case that the initial neural breakdown associated with stuttering occurs in L-IFG—during the planning phase, as indicated by the planning contrast results—and that R-IFG and R-SMG support awareness of this disruption and the simultaneous decision-making related to how to respond to it. This claim warrants further investigation in light of the fact that the speech of the AWS in this study was perceptually fluent, and it was impossible to determine whether there was anticipation at all. Still, future investigations might include the extension of previous methods to elicit anticipation during neuroimaging (den Ouden, Montgomery, & Adams, 2013; Wymbs, Ingham, Ingham, Paolini, & Grafton, 2013) allowing for a comparison between anticipated and un-anticipated stuttering.

Sensorimotor integration difficulty in adults who stutter

An additional finding of interest is that the AWS exhibited greater activation in R-postCG during the overt vs. covert condition, as well as greater activation in R-postCG compared to the CON during the overt condition. R-postCG includes somatosensory cortex, a region important for the online integration of sensory (acoustic, kinesthetic, proprioceptive) information and therefore critically important to fluent speech production (Guenther, 2016). Atypical activity in R-postCG reveals a possible neural correlate for the sensorimotor integration difficulty exhibited by AWS during speech production (S. Cai, Beal, Ghosh, Guenther, & Perkell, 2014; Daliri, Wieland, Cai, Guenther, & Chang, 2018; T. M. Loucks & De Nil, 2006; T. M. Loucks, De Nil, & Sasisekaran, 2007). That AWS exhibit greater activity than CON suggests over-activation in these somatosensory areas during speech production, which may result from increased sensitivity in these regions. Alternatively, AWS may exhibit an overreliance on somatosensory feedback (Max, Guenther, Gracco, Ghosh, & Wallace, 2004), and as a result, activation is boosted in this area during overt speech production. This would be in line with computational simulations that show that AWS rely on a motor strategy that is weighted excessively toward feedback mechanisms (Civier, Tasko, & Guenther, 2010).

Alignment with previous PET/fMRI results

In the present study, we used an innovative image-based approach to fNIRS research that allowed us to analyze neural activity within the brain volume. This has the advantage of direct comparisons with previous PET/fMRI research. The group-level results are in agreement with previous fMRI/PET studies that show widespread differences between AWS and CON in bilateral frontal, motor, parietal, and temporal network activation patterns during the overt and covert production of single words or

short utterances (Chang et al., 2009; De Nil et al., 2008, 2000; T. Loucks et al., 2011; Lu, Chen, et al., 2010; Lu et al., 2009; Lu, Peng, et al., 2010). Although there are important planning versus execution task-based differences, in general the AWS exhibited over-activation in right hemisphere regions including R-IFG, R-MFG, R-postCG, and R-SMG, and under-activation in left hemisphere networks including L-IFG, and L-pre- and postCG for simple non-word and word production.

These findings provide support that fNIRS is a suitable alternative to PET/fMRI for localizing cortical activity during the speech production of single words or short utterances in AWS. fNIRS offers several advantages over fMRI including cost, efficiency, portability, and the possibility of investigating speech production in naturalistic testing environments (e.g., sitting upright, face-to-face), which is especially relevant because stuttering primarily emerges during communicative (and not non-communicative) speech. Future studies should leverage these advantages. Note that one limitation of the present approach to image-reconstruction is that our method does not allow for an examination of the time-course of the fNIRS signals within the brain volume. We did a limited examination of this issue in the present study, showing good correspondence between a channel-based analysis of HbO and the volumetric group main effect; however, more work is needed on this front. For instance, our group is currently comparing the image-reconstruction approach used here with the approach developed by Eggebrecht et al. [ref]. An advantage of the latter approach is that it retains time-course information when reconstructing the fNIRS signal within the brain volume.

Limitations

Although we followed the rationale of Lu et al. (2010) and focused on speech motor aspects of production, linguistic features such as wordlikeness and prosody may have confounded our interpretation of the planning results. That is, the SSN and DSN may have differed with regard to these features. Future work should more closely examine the impact that wordlikeness and prosody have on stuttering. In addition, the execution task may have functioned as a “go-no-go” task such that inhibition was ongoing during the covert trials. It should be emphasized, however, that participants were explicitly instructed to say the words in their heads (i.e., without articulation), and because all of the words were simple we assumed that all of the participants followed these instructions correctly. In this way, the task was not a true “go-no-go” task in that participants still “said” the word but without articulation. Future investigations should more closely examine the impact of inhibition on speech execution.

The results from this study illuminate key differences between planning and execution processing in AWS. Specifically, increases in planning load resulted in atypical neural activation in the L-IFG in AWS whereas increases in execution load resulted in atypical neural activation in right fronto-temporo-parietal and motor regions. Future work should investigate planning and execution in children who stutter, as well as during more ecologically realistic conditions (e.g., social interaction). In addition, we contribute to a limited literature on fNIRS and stuttering by corroborating previous PET/fMRI results and further demonstrate the feasibility and benefits of using fNIRS technology in stuttering research. In particular, the ecological validity of the data that can be collected using fNIRS is especially important for the study of stuttering which primarily emerges during interactive communicative contexts.

Contributors

BB, TZ, JPS and SW designed the study for BB's dissertation. BB collected the data. SW, BB, JPS, and ESJ analyzed the data. ESJ, SW, JPS, DSB, and TZ interpreted the results and wrote the manuscript.

Acknowledgments

The DeLTA Center at the University of Iowa supported collection of the fNIRS data. Preparation of this manuscript was supported by NSF SBE 1513770 awarded to Eric S. Jackson.

Conflicts of interest

There are no conflicts of interest.

References

- Adlington, R. L., Laws, K. R., & Gale, T. M. (2009). The Hatfield Image Test (HIT): A new picture test and norms for experimental and clinical use. *Journal of Clinical and Experimental Neuropsychology*, *31*(6), 731–753.
- Aron, A. R., Behrens, T. E., Smith, S., Frank, M. J., & Poldrack, R. A. (2007). Triangulating a cognitive control network using diffusion-weighted magnetic resonance imaging (MRI) and functional MRI. *Journal of Neuroscience*, *27*(14), 3743–3752.
- Aron, A. R., & Poldrack, R. A. (2006). Cortical and subcortical contributions to stop signal response inhibition: role of the subthalamic nucleus. *Journal of Neuroscience*, *26*(9), 2424–2433.
- Aron, A. R., Robbins, T. W., & Poldrack, R. A. (2004). Inhibition and the right inferior frontal cortex. *Trends in Cognitive Sciences*, *8*(4), 170–177.
- Arrington, C. M., Carr, T. H., Mayer, A. R., & Rao, S. M. (2000). Neural Mechanisms of Visual Attention: Object-Based Selection of a Region in Space. *Journal of Cognitive Neuroscience*, *12*(supplement 2), 106–117. <https://doi.org/10.1162/089892900563975>
- Beal, D. S., Gracco, V. L., Brettschneider, J., Kroll, R. M., & Luc, F. (2013). A voxel-based morphometry (VBM) analysis of regional grey and white matter volume abnormalities within the speech production network of children who stutter. *Cortex*, *49*(8), 2151–2161.
- Beal, D. S., Lerch, J. P., Cameron, B., Henderson, R., Gracco, V. L., & De Nil, L. F. (2015). The trajectory of gray matter development in Broca's area is abnormal in people who stutter. *Frontiers in Human Neuroscience*, *9*, 89.
- Beilby, J. M., Byrnes, M. L., Meagher, E. L., & Yaruss, J. S. (2013). The impact of stuttering on adults who stutter and their partners. *Journal of Fluency Disorders*, *38*(1), 14–29.
- Bohland, J. W., & Guenther, F. H. (2006). An fMRI investigation of syllable sequence production. *Neuroimage*, *32*(2), 821–841.
- Braun, A. R., Varga, M., Stager, S., Schulz, G., Selbie, S., Maisog, J. M., ... Ludlow, C. L. (1997). Altered patterns of cerebral activity during speech and language production in developmental stuttering. An H2 (15) O positron emission tomography study. *Brain*, *120*(5), 761–784.
- Brown, S., Ingham, R. J., Ingham, J. C., Laird, A. R., & Fox, P. T. (2005). Stuttered and fluent speech production: an ALE meta-analysis of functional neuroimaging studies. *Human Brain Mapping*, *25*(1), 105–117.
- Budde, K. S., Barron, D. S., & Fox, P. T. (2014). Stuttering, induced fluency, and natural fluency: A hierarchical series of activation likelihood estimation meta-analyses. *Brain and Language*, *139*, 99–107.
- Cai, S., Beal, D. S., Ghosh, S. S., Guenther, F. H., & Perkell, J. S. (2014). Impaired timing adjustments in response to time-varying auditory perturbation during connected speech production in persons who stutter. *Brain and Language*, *129*, 24–29. <https://doi.org/10.1016/j.bandl.2014.01.002>
- Cai, W., Ryali, S., Chen, T., Li, C.-S. R., & Menon, V. (2014). Dissociable Roles of Right Inferior Frontal Cortex and Anterior Insula in Inhibitory Control: Evidence from Intrinsic and Task-Related Functional Parcellation, Connectivity, and Response Profile Analyses across Multiple Datasets. *Journal of Neuroscience*, *34*(44), 14652–14667. <https://doi.org/10.1523/JNEUROSCI.3048-14.2014>
- Chang, S.-E., Erickson, K. I., Ambrose, N. G., Hasegawa-Johnson, M. A., & Ludlow, C. L. (2008). Brain anatomy differences in childhood stuttering. *Neuroimage*, *39*(3), 1333.

- Chang, S.-E., Horwitz, B., Ostuni, J., Reynolds, R., & Ludlow, C. L. (2011). Evidence of left inferior frontal–premotor structural and functional connectivity deficits in adults who stutter. *Cerebral Cortex*, *21*(11), 2507–2518.
- Chang, S.-E., Kenney, M. K., Loucks, T. M., & Ludlow, C. L. (2009). Brain activation abnormalities during speech and non-speech in stuttering speakers. *Neuroimage*, *46*(1), 201.
- Chesters, J., Möttönen, R., & Watkins, K. E. (2018). Transcranial direct current stimulation over left inferior frontal cortex improves speech fluency in adults who stutter. *Brain*.
- Civier, O., Tasko, S. M., & Guenther, F. H. (2010). Overreliance on auditory feedback may lead to sound/syllable repetitions: simulations of stuttering and fluency-inducing conditions with a neural model of speech production. *Journal of Fluency Disorders*, *35*(3), 246–279.
- Corbetta, M., Kincade, J. M., Ollinger, J. M., McAvo, M. P., & Shulman, G. L. (2000). Voluntary orienting is dissociated from target detection in human posterior parietal cortex. *Nature Neuroscience*, *3*(3), 292.
- Corbetta, M., Kincade, J. M., & Shulman, G. L. (2002). Neural systems for visual orienting and their relationships to spatial working memory. *Journal of Cognitive Neuroscience*, *14*(3), 508–523.
- Craig, A., Blumgart, E., & Tran, Y. (2009). The impact of stuttering on the quality of life in adults who stutter. *Journal of Fluency Disorders*, *34*(2), 61–71.
- Daliri, A., Wieland, E. A., Cai, S., Guenther, F. H., & Chang, S.-E. (2018). Auditory-motor adaptation is reduced in adults who stutter but not in children who stutter. *Developmental Science*, *21*(2), e12521.
- De Nil, L. F., Beal, D. S., Lafaille, S. J., Kroll, R. M., Crawley, A. P., & Gracco, V. L. (2008). The effects of simulated stuttering and prolonged speech on the neural activation patterns of stuttering and nonstuttering adults. *Brain and Language*, *107*(2), 114–123.
- De Nil, L. F., Kroll, R. M., Kapur, S., & Houle, S. (2000). A positron emission tomography study of silent and oral single word reading in stuttering and nonstuttering adults. *Journal of Speech, Language and Hearing Research*, *43*(4), 1038.
- De Nil, L. F., Kroll, R. M., Lafaille, S. J., & Houle, S. (2004). A positron emission tomography study of short-and long-term treatment effects on functional brain activation in adults who stutter. *Journal of Fluency Disorders*, *28*(4), 357–380.
- den Ouden, D.-B., Montgomery, A., & Adams, C. (2013). Simulating the neural correlates of stuttering. *Neurocase*, *20*(4), 434–445.
- Dravida, S., Noah, J. A., Zhang, X., & Hirsch, J. (2017). Comparison of oxyhemoglobin and deoxyhemoglobin signal reliability with and without global mean removal for digit manipulation motor tasks. *Neurophotonics*, *5*(1), 11006.
- Eggebrecht, A. T., Ferradal, S. L., Robichaux-Viehoever, A., Hassanpour, M. S., Dehghani, H., Snyder, A. Z., ... Culver, J. P. (2014). Mapping distributed brain function and networks with diffuse optical tomography. *Nature Photonics*, *8*(6), 448.
- Ferrari, M., & Quaresima, V. (2012). A brief review on the history of human functional near-infrared spectroscopy (fNIRS) development and fields of application. *Neuroimage*, *63*(2), 921–935.
- Fox, P. T., Ingham, R. J., Ingham, J. C., Zamarripa, F., Xiong, J.-H., & Lancaster, J. L. (2000). Brain correlates of stuttering and syllable production A PET performance-correlation analysis. *Brain*, *123*(10), 1985–2004.
- Garnett, E. O., Chow, H. M., Nieto-Castañón, A., Tourville, J. A., Guenther, F. H., & Chang, S.-E. (2018). Anomalous morphology in left hemisphere motor and premotor cortex of children

- who stutter. *Brain*, 141(9), 2670–2684.
- Guenther, F. H. (2016). *Neural Control of Speech*. MIT Press.
- Hartwigsen, G., Neef, N. E., Camilleri, J. A., Margulies, D. S., & Eickhoff, S. B. (2018). Functional Segregation of the Right Inferior Frontal Gyrus: Evidence From Coactivation-Based Parcellation. *Cerebral Cortex*.
- Heim, S., Eickhoff, S. B., & Amunts, K. (2009). Different roles of cytoarchitectonic BA 44 and BA 45 in phonological and semantic verbal fluency as revealed by dynamic causal modelling. *Neuroimage*, 48(3), 616–624.
- Hirsch, J., Adam Noah, J., Zhang, X., Dravida, S., & Ono, Y. (2018). A cross-brain neural mechanism for human-to-human verbal communication. *Social Cognitive and Affective Neuroscience*, 13(9), 907–920.
- Indefrey, P., & Levelt, W. J. (2004). The spatial and temporal signatures of word production components. *Cognition*, 92(1–2), 101–144.
- Jackson, E. S., Yaruss, J. S., Quesal, R. W., Terranova, V., & Whalen, D. H. (2015). Responses of adults who stutter to the anticipation of stuttering. *Journal of Fluency Disorders*, 45, 38–51.
- Jiang, J., Lu, C., Peng, D., Zhu, C., & Howell, P. (2012). Classification of Types of Stuttering Symptoms Based on Brain Activity. *PloS One*, 7(6), e39747.
- Johnson, W., Darley, F. L., & Spriesterbach, D. C. (1963). Scale for rating severity of stuttering. In *Diagnostic methods in speech pathology* (p. 281).
- Kell, C. A., Neumann, K., von Kriegstein, K., Posenenske, C., von Gudenberg, A. W., Euler, H., & Giraud, A.-L. (2009). How the brain repairs stuttering. *Brain*, 132(10), 2747–2760.
- Kronfeld-Duenias, V., Amir, O., Ezrati-Vinacour, R., Civier, O., & Ben-Shachar, M. (2016). The frontal aslant tract underlies speech fluency in persistent developmental stuttering. *Brain Structure & Function*, 221(1), 365–381. <https://doi.org/10.1007/s00429-014-0912-8>
- Loucks, T., Kraft, S. J., Choo, A. L., Sharma, H., & Ambrose, N. G. (2011). Functional brain activation differences in stuttering identified with a rapid fMRI sequence. *Journal of Fluency Disorders*, 36(4), 302–307.
- Loucks, T. M., & De Nil, L. F. (2006). Anomalous sensorimotor integration in adults who stutter: A tendon vibration study. *Neuroscience Letters*, 402(1), 195–200.
- Loucks, T. M., De Nil, L. F., & Sasisekaran, J. (2007). Jaw-phonatory coordination in chronic developmental stuttering. *Journal of Communication Disorders*, 40(3), 257–272.
- Lu, C., Chen, C., Ning, N., Ding, G., Guo, T., Peng, D., ... Lin, C. (2010). The neural substrates for atypical planning and execution of word production in stuttering. *Experimental Neurology*, 221(1), 146–156.
- Lu, C., Ning, N., Peng, D., Ding, G., Li, K., Yang, Y., & Lin, C. (2009). The role of large-scale neural interactions for developmental stuttering. *Neuroscience*, 161(4), 1008–1026.
- Lu, C., Peng, D., Chen, C., Ning, N., Ding, G., Li, K., ... Lin, C. (2010). Altered effective connectivity and anomalous anatomy in the basal ganglia-thalamocortical circuit of stuttering speakers. *Cortex*, 46(1), 49–67.
- Max, L., Guenther, F. H., Gracco, V. L., Ghosh, S. S., & Wallace, M. E. (2004). Unstable or insufficiently activated internal models and feedback-biased motor control as sources of dysfluency: A theoretical model of stuttering. *Contemporary Issues in Communication Science and Disorders*, 31, 105–122.
- Misaghi, E., Zhang, Z., Gracco, V. L., Luc, F., & Beal, D. S. (2018). White matter tractography of the neural network for speech-motor control in children who stutter. *Neuroscience Letters*, 668, 37–42.

- Mooshammer, C., Goldstein, L., Nam, H., McClure, S., Saltzman, E., & Tiede, M. (2012). Bridging planning and execution: Temporal planning of syllables. *Journal of Phonetics*, *40*(3), 374–389.
- Neef, N. E., Anwander, A., Bütfering, C., Schmidt-Samoa, C., Friederici, A. D., Paulus, W., & Sommer, M. (2018). Structural connectivity of right frontal hyperactive areas scales with stuttering severity. *Brain*, *141*(1), 191–204. <https://doi.org/10.1093/brain/awx316>
- Neumann, K., Euler, H. A., Gudenberg, A. W. von, Giraud, A.-L., Lanfermann, H., Gall, V., & Preibisch, C. (2004). The nature and treatment of stuttering as revealed by fMRI: A within-and between-group comparison. *Journal of Fluency Disorders*, *28*(4), 381–410.
- Neumann, K., Euler, H. A., von Gudenberg, A. W., Giraud, A.-L., Lanfermann, H., Gall, V., & Preibisch, C. (2003). The nature and treatment of stuttering as revealed by fMRI: A within-and between-group comparison. *Journal of Fluency Disorders*, *28*(4), 381–410.
- Papoutsis, M., de Zwart, J. A., Jansma, J. M., Pickering, M. J., Bednar, J. A., & Horwitz, B. (2009). From phonemes to articulatory codes: an fMRI study of the role of Broca's area in speech production. *Cerebral Cortex*, *19*(9), 2156–2165.
- Perlman, S. B., Huppert, T. J., & Luna, B. (2015). Functional near-infrared spectroscopy evidence for development of prefrontal engagement in working memory in early through middle childhood. *Cerebral Cortex*, *26*(6), 2790–2799.
- Perlman, S. B., Huppert, T. J., & Luna, B. (2016). Functional Near-Infrared Spectroscopy Evidence for Development of Prefrontal Engagement in Working Memory in Early Through Middle Childhood. *Cerebral Cortex (New York, NY)*, *26*(6), 2790–2799. <https://doi.org/10.1093/cercor/bhv139>
- Preibisch, C., Neumann, K., Raab, P., Euler, H. A., von Gudenberg, A. W., Lanfermann, H., & Giraud, A.-L. (2003). Evidence for compensation for stuttering by the right frontal operculum. *Neuroimage*, *20*(2), 1356–1364.
- Price, C. J. (2012). A review and synthesis of the first 20 years of PET and fMRI studies of heard speech, spoken language and reading. *Neuroimage*, *62*(2), 816–847.
- Putt, S. S., Wijekumar, S., Franciscus, R. G., & Spencer, J. P. (2017). The functional brain networks that underlie Early Stone Age tool manufacture. *Nature Human Behaviour*, *1*(6), 102.
- Qiao, J., Wang, Z., Zhao, G., Huo, Y., Herder, C. L., Sikora, C. O., & Peterson, B. S. (2017). Functional neural circuits that underlie developmental stuttering. *PloS One*, *12*(7), e0179255.
- Riecker, A., Brendel, B., Ziegler, W., Erb, M., & Ackermann, H. (2008). The influence of syllable onset complexity and syllable frequency on speech motor control. *Brain and Language*, *107*(2), 102–113. <https://doi.org/10.1016/j.bandl.2008.01.008>
- Sakai, N., Masuda, S., Shimotomai, T., & Mori, K. (2009). Brain activation in adults who stutter under delayed auditory feedback: An fMRI study. *International Journal of Speech-Language Pathology*, *11*(1), 2–11.
- Salmelin, R., Schnitzler, A., Schmitz, F., & Freund, H.-J. (2000). Single word reading in developmental stutterers and fluent speakers. *Brain*, *123*(6), 1184–1202.
- Schuhmann, T., Schiller, N. O., Goebel, R., & Sack, A. T. (2009). The temporal characteristics of functional activation in Broca's area during overt picture naming. *Cortex*, *45*(9), 1111–1116.
- Shuster, L. I., & Lemieux, S. K. (2005). An fMRI investigation of covertly and overtly produced mono-and multisyllabic words. *Brain and Language*, *93*(1), 20–31.
- Sörös, P., Sokoloff, L. G., Bose, A., McIntosh, A. R., Graham, S. J., & Stuss, D. T. (2006). Clustered functional MRI of overt speech production. *NeuroImage*, *32*(1), 376–387. <https://doi.org/10.1016/j.neuroimage.2006.02.046>

- Strangman, G., Culver, J. P., Thompson, J. H., & Boas, D. A. (2002). A quantitative comparison of simultaneous BOLD fMRI and NIRS recordings during functional brain activation. *Neuroimage*, *17*(2), 719–731.
- Tellis, G. M., Vitale, C., & Murgallis, T. (2015). Near infrared spectroscopy (NIRS): A pilot study to measure hemoglobin concentration changes in the brains of persons who stutter and typically fluent speakers. *Procedia-Social and Behavioral Sciences*, *193*, 261–265.
- Vanderhasselt, M.-A., Kühn, S., & De Raedt, R. (2013). “Put on your poker face”: neural systems supporting the anticipation for expressive suppression and cognitive reappraisal. *Social Cognitive and Affective Neuroscience*, *8*(8), 903–910. <https://doi.org/10.1093/scan/nss090>
- Vitevitch, M., & Luce, P. (2004). A Web-based interface to calculate phonotactic probability for words and nonwords in English. *Behavior Research Methods, Instruments, & Computers : A Journal of the Psychonomic Society, Inc*, *36*(3), 481–487.
- Walsh, B., Tian, F., Tourville, J. A., Yücel, M. A., Kuczek, T., & Bostian, A. J. (2017). Hemodynamics of speech production: An fNIRS investigation of children who stutter. *Scientific Reports*, *7*. Retrieved from <https://www.ncbi.nlm.nih.gov/pmc/articles/PMC5481456/>
- Watkins, K. E., Smith, S. M., Davis, S., & Howell, P. (2008). Structural and functional abnormalities of the motor system in developmental stuttering. *Brain*, *131*(1), 50–59.
- Wijekumar, S., Huppert, T. J., Magnotta, V. A., Buss, A. T., & Spencer, J. P. (2017). Validating an image-based fNIRS approach with fMRI and a working memory task. *NeuroImage*, *147*, 204–218.
- Wijekumar, S., Magnotta, V. A., & Spencer, J. P. (2017). Modulating perceptual complexity and load reveals degradation of the visual working memory network in ageing. *NeuroImage*, *157*, 464–475.
- Wijekumar, S., Spencer, J. P., Bohache, K., Boas, D. A., & Magnotta, V. A. (2015). Validating a new methodology for optical probe design and image registration in fNIRS studies. *Neuroimage*, *106*, 86–100.
- Wymbs, N. F., Ingham, R. J., Ingham, J. C., Paolini, K. E., & Grafton, S. T. (2013). Individual differences in neural regions functionally related to real and imagined stuttering. *Brain and Language*, *124*(2), 153–164.
- Yada, Y., Tomisato, S., & Hashimoto, R. (2018). Online cathodal transcranial direct current stimulation to the right homologue of Broca’s area improves speech fluency in people who stutter. *Psychiatry and Clinical Neurosciences*.
- Yairi, E., & Ambrose, N. (1992). A Longitudinal Study of Stuttering in Children. *Journal of Speech, Language, and Hearing Research*, *35*(4), 755–760.
- Yücel, M. A., Selb, J., Cooper, R. J., & Boas, D. A. (2014). Targeted principle component analysis: a new motion artifact correction approach for near-infrared spectroscopy. *Journal of Innovative Optical Health Sciences*, *7*(2), 1350066.
- Zhang, X., Noah, J. A., Dravida, S., & Hirsch, J. (2017). Signal processing of functional NIRS data acquired during overt speaking. *Neurophotonics*, *4*(4), 41409.
- Zhang, X., Noah, J. A., & Hirsch, J. (2016). Separation of the global and local components in functional near-infrared spectroscopy signals using principal component spatial filtering. *Neurophotonics*, *3*(1), 15004–15004.

Region	Hemi	Center of Mass (MNI coordinates)			Chrom	Size (mm ³)	F-statistic		Effect Size (d)
		x	y	z			Mean	SEM	
Group									
postCG	R	-60	3.4	28.7	HbO	680	4.9	0.06	.36
MFG	R	-48.2	-20.8	38.9	HbR	280	4.7	0.06	.05
SMG	R	-53.2	28.9	47.3	HbR	248	6.1	0.26	.22
IFG	L	54.5	-36.5	6.7	HbR	176	4.6	0.05	.18
MFG	R	-45.5	-28.4	40.7	HbO	168	5.1	0.17	.88
IFG	L	56.5	-38.2	5.1	HbO	104	5.5	0.23	.30
Group X Condition									
IFG	L	56	-6.8	11	HbR	656	4.6	0.03	.20
MFG	L	37.9	-9.5	50.4	HbO	408	5.2	0.1	.18
IFG	R	-51.1	-18.8	17.3	HbO	136	5.6	0.31	.21

Region	Hemi	Center of Mass (MNI coordinates)			Chrom	Size (mm ³)	F-statistic		Effect Size (d)
		x	y	z			Mean	SEM	
Group									
IFG	R	-50.7	-24	25	HbO	3128	6	0.08	.67
SMG	R	-59.4	43.3	30.8	HbR	1368	5.1	0.05	.07
preCG	L	58.2	1.9	27.9	HbR	936	4.8	0.03	.30
postCG	L	19.3	30.5	71.9	HbR	872	4.5	0.02	.70
preCG	R	-37.6	8.6	59.1	HbO	848	5.2	0.06	.52
postCG	L	61.7	15.1	15.8	HbO	568	4.6	0.03	.23
IFG	R	-56.3	-17	20.1	HbR	376	4.7	0.06	.35
MFG	R	-39.4	-7.6	52.6	HbR	360	4.7	0.05	.55
SMG	L	53.8	20.6	42.1	HbR	280	4.9	0.1	.16
IFG	L	60.9	-8.7	19.1	HbO	264	5.8	0.25	.20
SMA	R	-4.5	11.7	63	HbO	160	4.7	0.07	.38
postCG	R	-38.7	34.8	64.2	HbR	136	4.7	0.08	.42
preCG	R	-32.6	22.6	71.5	HbR	104	5	0.17	.21
Group X Condition									
postCG	R	-58.4	18.6	33.5	HbR	872	5.3	0.09	.04
SMG	R	-63.2	24.2	19.2	HbO	768	4.7	0.03	.01
preCG	L	30.8	26.8	65.8	HbR	360	4.8	0.07	.45
STG	R	-61.5	0.6	-0.8	HbO	232	4.7	0.06	.08
preCG	L	47.2	-0.9	41.3	HbR	120	4.5	0.05	.05
preCG	L	53.7	-4	44.5	HbR	120	4.6	0.04	.06
preCG	L	60.7	-3.9	29.1	HbR	112	4.4	0.09	.36
IFG	R	-54.9	-22.6	-0.2	HbO	104	4.5	0.08	.09

Captions

Figure 1. Visual depiction of one trial from the planning (top) and execution (bottom) tasks. For the planning task, participants viewed the fixation mark, heard the non-word, produced the non-word, and rested for the jittered inter-stimulus interval of two, four, or six seconds. For the execution task, participants viewed the fixation mark, followed by the picture, were presented with the “go” signal to either produce the word overtly (green frame) or covertly (red frame), and then rested for the jittered inter-stimulus interval of two, four, or six seconds.

Figure 2. Probe geometry. (A) Source (red) and detector (blue) probe geometry for one participant projected onto an age-specific atlas. (B) Sensitivity profiles for the same participant resultant of Monte Carlo simulations with 100 million photons. (C) Three dimensional reconstruction of the group mask.

Table 1. Group main effects and interactions for the planning task. HbO = oxygenated hemoglobin; Hemi = Hemisphere; Chrom = Chromophores; HbR = deoxygenated hemoglobin; postCG = postcentral gyrus; IFG = inferior frontal gyrus; MFG = middle frontal gyrus; SMG = supramarginal gyrus; SEM = standard error of the mean.

Table 2. Group main effects and interactions for execution task. Hemi = Hemisphere; Chrom = Chromophores; HbO = oxygenated hemoglobin; HbR = deoxygenated hemoglobin; IFG = inferior frontal gyrus; SMG = supramarginal gyrus; preCG = precentral gyrus; postCG = postcentral gyrus; MFG = middle frontal gyrus; SMA = supplementary motor area; STG = superior temporal gyrus. SEM = standard error of the mean.

Figure 3. (A). Group main effects of the planning and execution tasks (combined). Green indicates AWS < CON; red indicates AWS > CON. Axial slice number in white. Images are presented in neurological convention (left is left). (B) Hemodynamic response functions (HRFs) for two example clusters (R-IFG, R-postCG; see text for details). IFG = inferior frontal gyrus; preCG = precentral gyrus; postCG = postcentral gyrus; SMG = supramarginal gyrus; MFG = middle frontal gyrus.

Figure 4. Statistically significant post-hoc comparisons for the planning (A) and execution (B) contrasts. For planning, dark green indicates CON, DSN

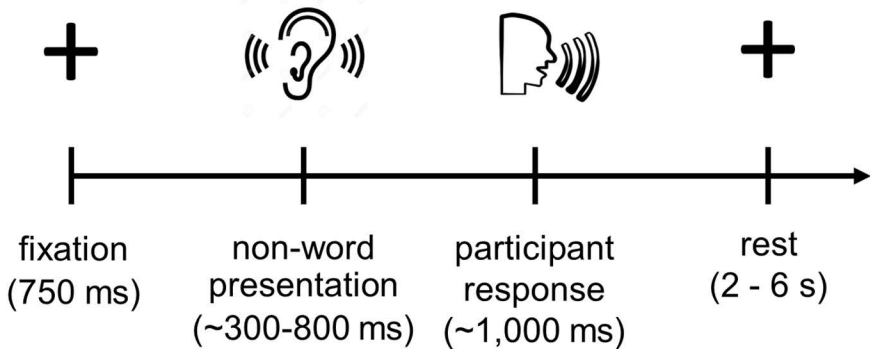
> SSN (high > low). For execution, purple indicates CON, covert > overt; red indicates AWS, covert > overt; light green indicates AWS, overt > covert. Axial slice number in white. Images are presented in neurological convention.

Appendix A. Planning task stimuli.

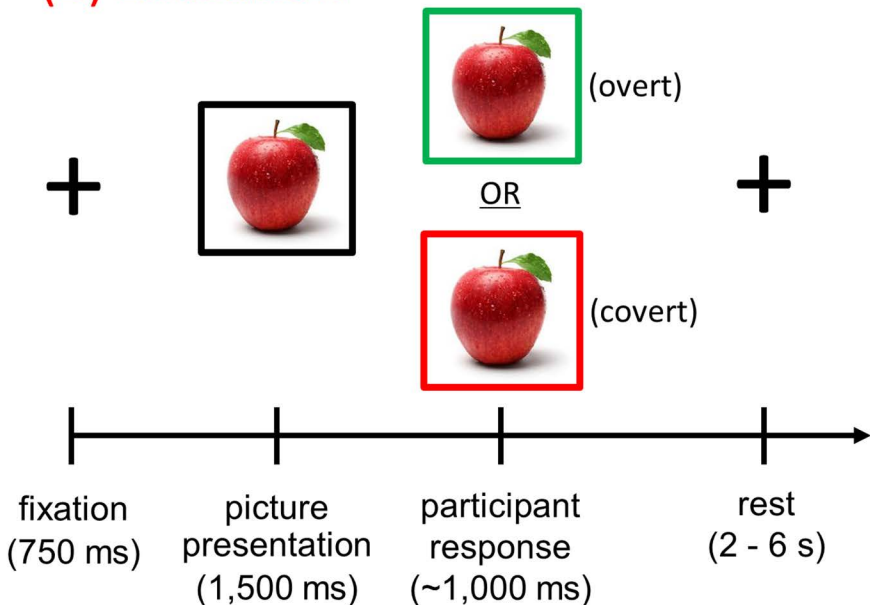
Appendix B. Execution task stimuli.

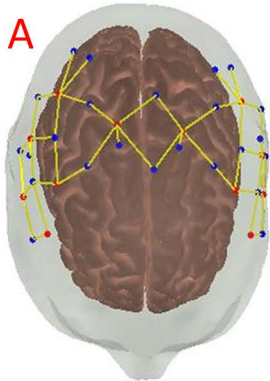
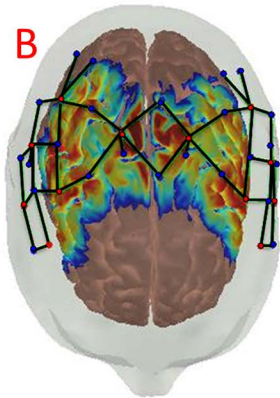
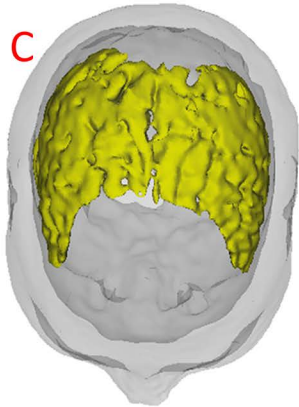
Appendix C. Condition main effects for both contrasts (planning and execution). HbO = oxygenated hemoglobin; HbR = deoxygenated hemoglobin; STG = superior temporal gyrus; postCG = postcentral gyrus; MFG = middle frontal gyrus; IFG = inferior frontal gyrus; RO = Rolandic operculum; preCG = precentral gyrus.

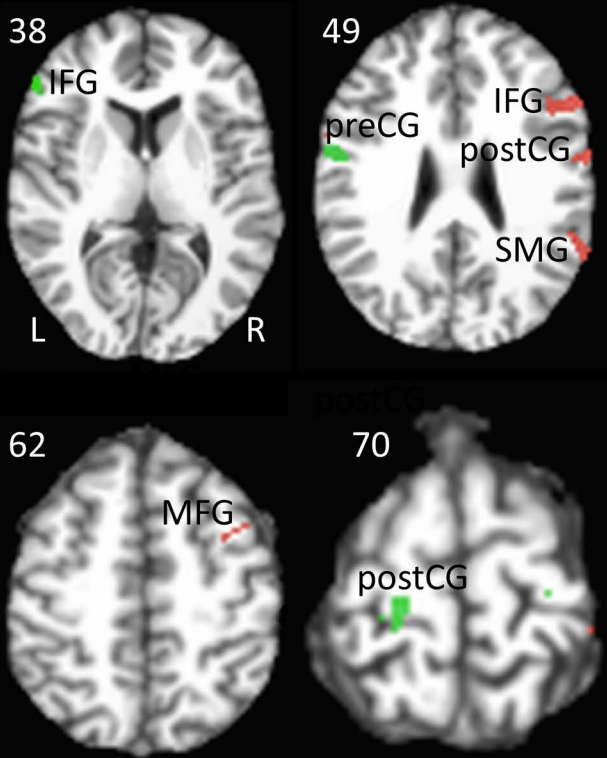
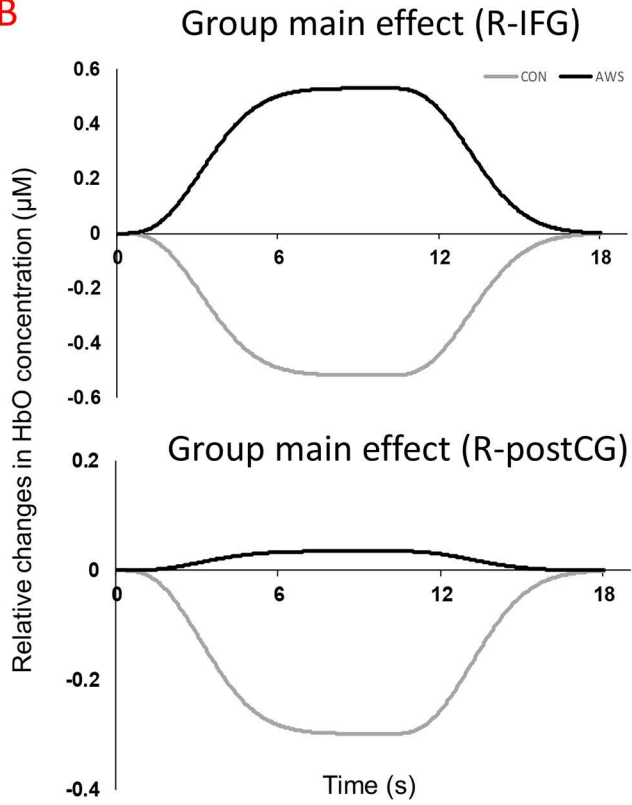
(A) Planning



(B) Execution

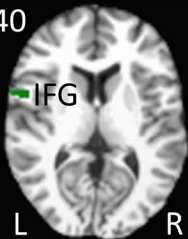


A**B****C**

A**B**

A

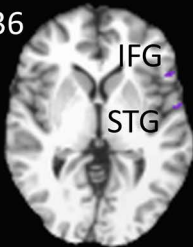
40



Planning

B

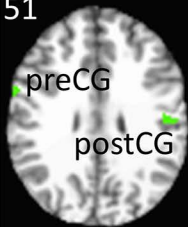
36



45



51



Execution

Same Syllable Non-words (SSN)	Different Syllable Non-words (DSN)
nauk nauk nauk	baseri
trod trod trod	grassbrellna
mump mump mump	stragensaur
soove soove soove	spinoball
fark fark fark	hambearfly
clus clus clus	ditabug
oom oom oom	poapus
huut huut huut	kangmaroo
horl horl horl	octager
florch florch florch	camgato
haith haith haith	bahadi
bot bot bot	betoper
laints laints laints	eldia
kade kade kade	dragegel
hote hote hote	laybera
bahs bahs bahs	camangfly
glau glau glau	toketo
fas fas fas	triterphant
koon koon koon	umnalope
kund kund kund	Babeli

Overt Naming	Covert Naming	Foil
apple	apple	
arm	arm	
banana	butterfly	*
basketball	basketball	
Bed	ball	
boat	boat	
broccoli	broccoli	
Bus	bus	
button	button	
camera	camera	
Car	car	
Cat	cat	
celery	celery	
cloud	hand	*
cookie	carrot	
couch	couch	
Cow	cow	
Cup	cup	
dinosaur	dinosaur	
dragonfly	octopus	*
duck	duck	
elephant	kangaroo	*
Eye	eye	
finger	giraffe	*
Fly	fly	
fork	fork	
grasshopper	grasshopper	
hamburger	hamburger	
horse	glove	*
house	house	
ladybug	ladybug	
moon	moon	
mouth	mouth	
pants	hat	*
potato	potato	
shoe	shoe	
shovel	shovel	
socks	lamp	*
table	table	
tomato	spaghetti	*
turtle	spider	*
umbrella	triangle	*

Region	Hemisphere	Center of Mass			Chrom	Size (mm ³)	F-statistic	
		x	y	z			Mean	SEM
Planning								
STG	R	-68.1	26.7	.5	HbR	480	4.8	.06
postCG	L	26.5	31.2	66.8	HbR	352	4.5	.04
STG	L	65.4	9.8	1.2	HbR	264	4.7	.06
MFG	R	-46.9	-23.4	42.6	HbR	208	4.6	.06
IFG	L	57	-37.5	4.3	HbR	96	4.9	.19
Execution								
Heschl's gyrus	R	59.8	2.5	-6.4	HbR	-6552	5.8	0.04
RO	L	60.7	-0.8	5.3	HbR	2136	5	0.03
IFG	R	-56	-8.9	19.5	HbO	2136	5.3	0.05
preCG	L	32.2	25.8	66.3	HbR	1320	7.1	0.17
postCG	L	60.1	14	18.1	HbR	1160	6.5	0.16
RO	L	59.7	-6.8	1.6	HbO	1088	5.3	0.19
postCG	R	-58.8	10	21.5	HbO	472	5.7	0.16
preCG	L	19.4	18.3	70.6	HbR	232	5.3	0.13
postCG	R	-38.7	38.1	68.6	HbO	112	4.9	0.09